An illustration of adaptive Marchenko imaging

Joost van der Neut[1], Kees Wapenaar[1], Jan Thorbecke[1], Evert Slob[1], and Ivan Vasconcelos[2]

Abstract

In Marchenko imaging, wavefields are retrieved at specified focal points in the subsurface through an iterative scheme derived from the multidimensional Marchenko equation. The method requires seismic-reflection data at the earth's surface (after free-surface multiple elimination) and an estimate of the direct wavefield from the surface to each focal point, which can be computed, for instance, in a macrovelocity model. In the first iteration, the direct wavefield is crosscorrelated with the reflection data. This operation is identical to inverse-wavefield extrapolation as is applied commonly in various imaging schemes, for instance, in reverse time migration (RTM). At each succeeding iteration, the result of the previous iteration is truncated in time and crosscorrelated with the reflection data again. To obtain a seismic image, a multidimensional deconvolution-based imaging condition can be applied to the retrieved wavefields. By this approach, both primary reflections and internal multiples contribute to the construction of the image. Alternatively, a crosscorrelation-based imaging condition can be used in which only the primary reflections are imaged and the contributions of internal multiples are subtracted. The latter strategy offers more flexibility because the subtraction of redatumed internal multiples can be implemented adaptively. Through this approach, the artifacts from internal multiples can be removed effectively from a conventional RTM image.

Introduction

A few years ago, an iterative scheme was introduced to retrieve wavefields in an unknown 1D acoustic medium from its single-sided reflection response (Broggini et al., 2012). Extended to 3D wave propagation, the scheme defines the core of a novel imaging methodology for seismic-reflection data that has been named Marchenko imaging (Wapenaar et al., 2014). In this methodology, internal multiples are no longer treated as undesired noise, but rather as signals that contribute to the retrieved reflectivity. Unlike various other methods such as full-wavefield inversion or full-wavefield migration, Marchenko imaging can be applied at any individual location in the subsurface without having to resolve the reflecting interfaces of the overburden. To achieve this goal, all upgoing and downgoing constituents of the seismic wavefields that have been emitted by each source at the surface are retrieved by solving the multidimensional Marchenko equation (Wapenaar et al., 2014). The seismic image is obtained by a multidimensional deconvolution of the retrieved upgoing wavefields with the downgoing wavefields and evaluating the result of this operation at zero delay time.

By using this imaging condition, accurate amplitudes are retrieved and imaging artifacts from internal multiples are avoided naturally (Wapenaar et al., 2014). The establishment of this methodology hinges on solving the Marchenko equation, which is done currently by iterative substitution. Although the theory of Marchenko imaging has been described recently by Wapenaar et al. (2014), the underlying mechanism by which the wavefields are constructed in the subsurface is quite complex, and further explanation is beneficial.

In this article, we explain Marchenko imaging at an intuitive level, following a similar type of analysis as in van der Neut et al. (2014). Because multidimensional crosscorrelations with the recorded data are at the core of this method, the main mechanism by which internal multiples are constructed is related closely to existing demultiple methods, such as those presented by Weglein et al. (1997). This analogy also has been mentioned by J. Sheiman (personal communication, 2014). However, Marchenko imaging is different from these methods in the way truncations are applied, namely, at one-way traveltimes in a redatumed data domain. Moreover, the Marchenko method naturally deals with all orders of internal multiples.

The underlying reasoning for the truncations is based on causality arguments (Wapenaar et al., 2014). In 1D media, these truncations allow for an exact retrieval of the upgoing and downgoing wavefields in the subsurface. Thus, true amplitudes can be retrieved even in the absence of a subsurface velocity model, given that the frequency content of the data is sufficiently broad with respect to the reflectivity series. In multidimensional media, however, these truncations are not always well defined, which can result in inevitable artifacts with the current implementation (van der Neut et al., 2014). Note that aforementioned methods suffer from similar limitations. Despite these limitations, encouraging results have been reported on Marchenko imaging, even in severely complex media (Behura et al., 2014).

To illustrate Marchenko imaging, we introduce a synthetic model of a reservoir embedded between two salt bodies (Figure 1a). At the surface, 161 sources and 161 receivers have been laid
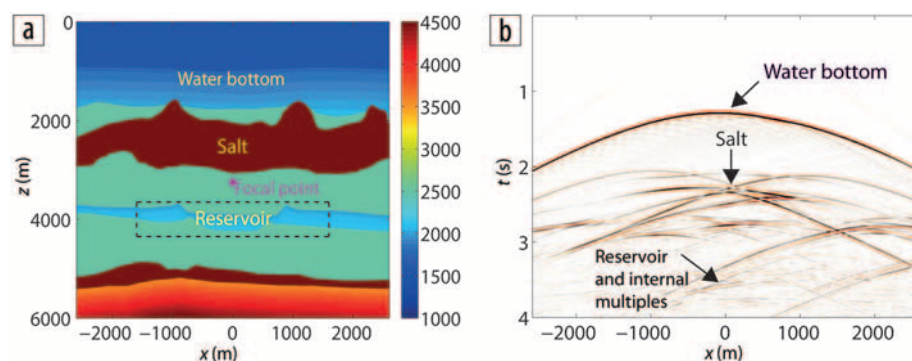

Figure 1. (a) Synthetic 2D model (colors indicate propagation velocity in meters per second). The magenta dot is a trial focal point. The dashed black box represents the target area. Model courtesy of Carlos Almagro Vidal. (b) Shot record for the central shot at x = 0 m.

Special Section: Multiples from attenuation to imaging

out on a fixed grid with 25-m spacing. Figure 1b shows the shot record of the central source at x = 0 m. The reflections and diffractions from the water bottom and the upper salt body have been indicated. Because of the low impedance contrasts (Figure 1a), the reflections from the reservoir are relatively weak and are covered by internal multiples from the overburden. This poses challenges for imaging the reservoir with conventional methodologies such as reverse time migration (RTM). Together, all 161 shot gathers constitute a data volume that we refer to as the reflection response.

Our aim is to retrieve the upgoing and downgoing wavefields that were emitted by each shot at the surface, as they would be recorded at a specified location in the subsurface that we call the focal point. In our example, a magenta dot indicates the focal point in Figure 1a. To retrieve the desired wavefields, we have to assume that an estimate of the so-called direct wavefield at the focal point is available. With the direct wavefield, we refer to that part of the total wavefield that reaches the focal point without any backscattering. Exact amplitudes can be retrieved if the direct wavefield is computed in the exact model. In practice, however, it is often sufficient to compute the wavefield in a smooth macrovelocity model, such as given in Figure 2a. In this example, we compute the direct wavefield by finite-difference modeling in the smooth model and display it in Figure 2b. Note the relative complexity of this wavefield, including multipathing arising from the complex salt structure.

Figure 2. (a) Smooth 2D model (colors indicate propagation velocity in meters per second) to compute the direct wavefield. (b) Direct wavefield at the focal point for all shot locations at the surface, computed in the smooth macrovelocity model. The green line denotes the truncation time that is applied in Marchenko imaging.

Figure 3. Illustration for the retrieval of various events during the first iteration: (a) an upgoing reflection at the focal point, (b) a focusing-function update, and (c) a spurious event. Note that crosscorrelation is applied by reversing the wavefield in time and convolution. Red rays indicate positive traveltimes, and green rays indicate negative traveltimes.

In Marchenko imaging, we take this estimate of the direct wavefield as an input to constitute the total upgoing and downgoing wavefields (including all orders of internal multiples) at the specified focal point. This is done by multiple multidimensional crosscorrelations with the reflection response, alternated with truncations. These truncations occur at a specified traveltime for each trace that is picked just before the first arrival of the direct wavefield. The green line in Figure 2b indicates these truncation times.

First iteration = inverse-wavefield extrapolation

In the first iteration of Marchenko imaging, the direct wavefield is crosscorrelated with the reflection data. This process can be visualized as reversing the direct wavefield in time and convolving it with these data. The result of this operation is identical to that of inverse-wav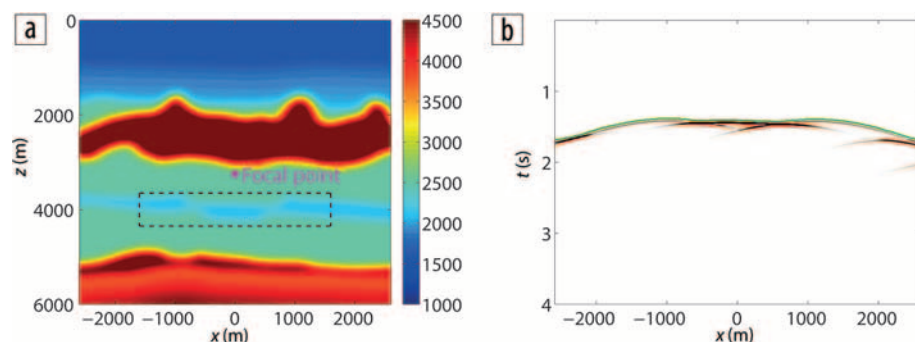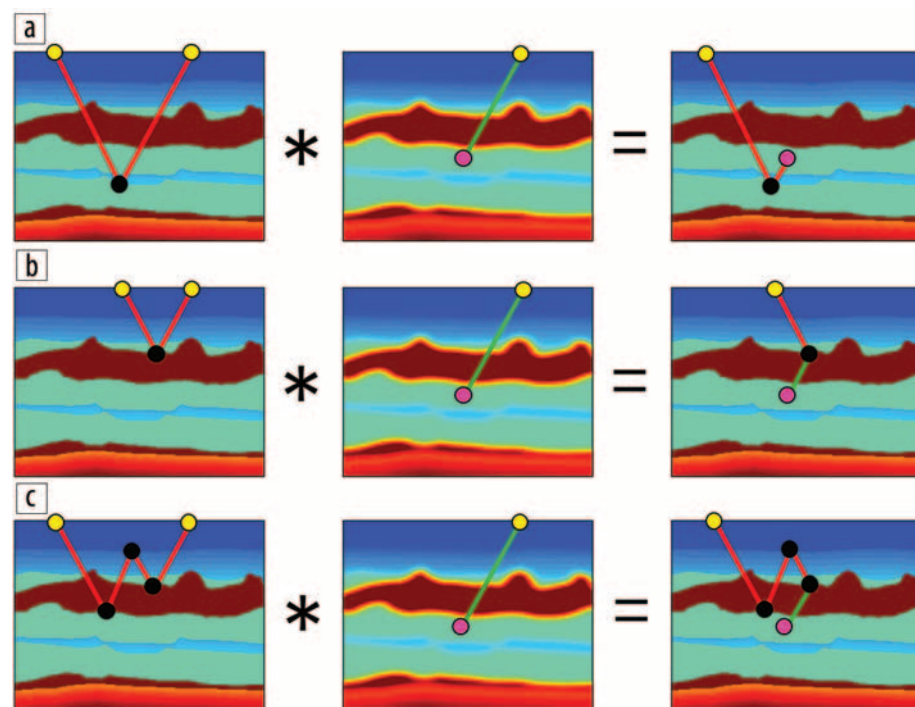efield extrapolation of the data from the surface to the focal point, as applied commonly in seismic redatuming and RTM (Schuster, 2002). Through the crosscorrelation process, the traveltime of the direct wavefield from the surface to the focal point is subtracted from the traveltimes of the recorded reflections, leaving the redatumed upgoing reflections at the focal point, as illustrated in Figure 3a.

In Figure 4a, we show the redatumed data after this operation. If the reflection response consisted solely of primary reflections from below the focal point, this response would be similar to the upgoing wavefield at the focal point, which we are after. For comparison, in Figure 4b, we computed the upgoing wavefield by finite-difference modeling and wavefield decomposition. When comparing Figures 4a and 4b, we observe that indeed, several primary reflections (for instance, those from the reservoir) have been retrieved correctly. However, we also observe various events in Figure 4a that cannot be observed in Figure
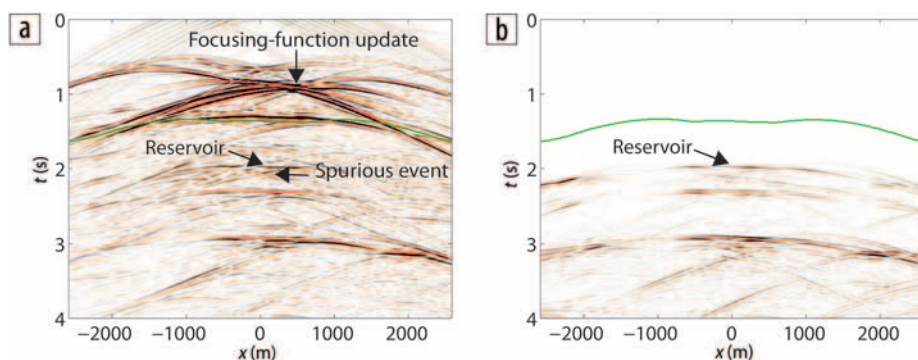
Figure 4. (a) Retrieved wavefield after the first iteration. (b) For comparison, the upgoing wavefield at the focal point for each source at the surface, computed by finite-difference modeling and wavefield decomposition. The green line denotes the truncation time used in Marchenko imaging.
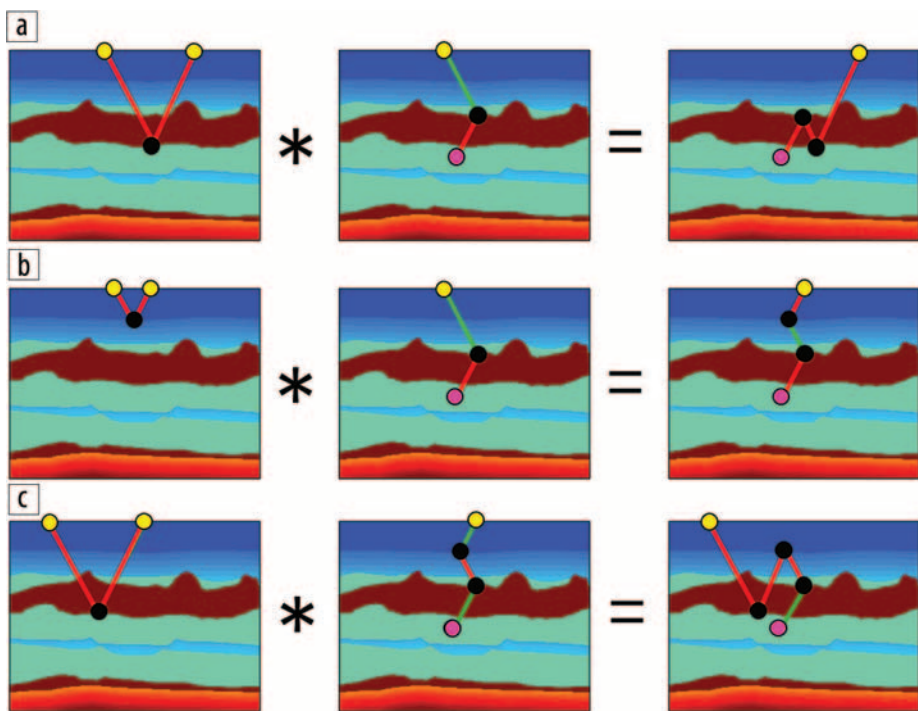

Figure 5. (a) Illustration for the retrieval of a downgoing reflection at the focal point during the second iteration. (b) A focusing-function update retrieved in the second iteration. (c) The focusing-function update retrieved in Figure 5b creates a counterevent during the third iteration, which is used to suppress the spurious event that appeared in Figure 3c. In all cases, the response of the previous iteration is truncated and crosscorrelated with the reflection response. Note that crosscorrelation is applied by reversing the wavefield in time and convolution. Red rays indicate positive traveltimes, and green rays indicate negative traveltimes.

event of the focusing function is generated in the first iteration. Akin to the generation of physical upgoing reflections, the traveltime of the direct wavefield from the surface to the focal point is subtracted from the recorded primary reflections. Besides the physical upgoing reflections and these focusing-function updates, we observe spurious events that arrive after the truncation time in Figure 4a. As an example, we illustrate in Figure 3c how such a spurious event is generated. This time, an internal-multiple reflection is crosscorrelated with the direct wavefield, yielding an event with an arrival time that exceeds the truncation time. Such a spurious event can obstruct an RTM image. However, the focusing-function updates can be used to mitigate this problem, which is achieved during subsequent iterations of Marchenko imaging.

Beyond reverse time migration

In conventional RTM, the recorded data are propagated backward in time and crosscorrelated with the source wavefield, which is propagated forward in time. As shown by Schuster (2002), RTM also can be implemented by redatuming the data to each focal point and crosscorrelating the result with the direct wavefield at that point. In Marchenko imaging, however, we go beyond RTM by updating the focusing function and crosscorrelating with the reflection response again. By doing this repeatedly, we update the downgoing wavefield at the focal point at the even iterations, while we update the upgoing wavefield at the odd iterations.

In Figure 5a, we illustrate how a focusing-function update (i.e., the time-reversed output of Figure 3b) from the first iteration produces a physical down-

4b. These events stem from the reflectors and diffractors above the focal point that are not accounted for by standard inverse-wavefield extrapolation. During later iterations of Marchenko imaging, they will be removed from the retrieved gathers.

The time-reversed direct wavefield that we have used to back-propagate the reflection data can be interpreted as an initial estimate of the so-called focusing function (Wapenaar et al., 2014). The focusing function is defined as a wavefield that focuses not only the primary reflections but also all orders of internal multiples at the focal point. At each iteration, the focusing function is updated with all events of the previous iteration that arrive before the truncation time. We have indicated these updates in Figure 4a. As an example, we illustrate in Figure 3b how an individual

going reflection when crosscorrelated with the reflection response in the second iteration. The amplitudes of these downgoing reflections are updated during later iterations, eventually leading to their exact values, as shown by Wapenaar et al. (2014) and various others. Besides downgoing reflections, new events emerge before the truncation time, as shown in Figure 5b. Once again, these events are used to update the focusing function. In Figure 5c, we show how these focusing-function updates are crosscorrelated with the data again in the third iteration, producing events with similar kinematics as the spurious events that appeared in the first iteration but with reversed polarity (compare the result of this operation with Figure 3c). Because of their opposite polarity, these events cancel the spurious events from the first iteration

Special Section: Multiples from attenuation to imaging

when the focusing-function updates are added together. Hence, we refer to them as counterevents.

To demonstrate this phenomenon, in Figure 6a, we show the update of the upgoing wavefield as retrieved at the third iteration. As indicated by the arrow, we can recognize several counterevents that have similar kinematics as the spurious events that we observed in Figure 4a (but with reversed polarity). Theoretically, it can be shown that the counterevents cancel the spurious events exactly when all odd iterations are added together (Wapenaar et al., 2014). However, this requires an accurately scaled reflection response, accurate knowledge of the source wavelet, accurate deghosting, and absence of noise and attenuation. In practice, we also can add each update with an adaptive filter, posing a minimum-energy criterion on the output gather. We emphasize that this can be done only for the upgoing wavefield and not for the downgoing wavefield. In Figure 6b, we have added adaptively the updates of the upgoing wavefield that we showed earlier (in Figures 4a and 6a). Note that the result is much closer to Figure 4b, being the true upgoing wavefield, and that the spurious events that appeared in Figure 4a have been suppressed successfully by this operation.

The imaging condition that was proposed by Wapenaar et al. (2014) involves a multidimensional deconvolution of the retrieved upgoing wavefield with the retrieved downgoing wavefield. This strategy results in a multiple-free image with accurate amplitudes, in which both primaries and internal multiples contribute. Alternatively, we can crosscorrelate the retrieved upgoing wavefield with the direct wavefield and evaluate the response at zero delay time. Such an imaging condition is similar to that of conventional RTM (Schuster, 2002), aiming solely at the imaging of primaries, not necessarily with accurate amplitudes. However, unlike in RTM, we can subtract spurious events prior to imaging, thereby improving the result.

To illustrate this advantage, we have applied RTM in a local target area around the reservoir indicated in Figure 1a. We show the conventional RTM image in Figure 7a. Although the reflectors have been positioned correctly, various artifacts exist. These artifacts are caused by the spurious events that appeared during inverse-wavefield extrapolation and contributed to the imaging condition at zero delay time, after crosscorrelation with the direct wavefield. In Figure 7b, we show that these artifacts are suppressed effectively when we use the upgoing wavefields predicted by the Marchenko scheme at each image point rather than the result of standard inverse-wavefield extrapolation. In this case, we have added only the first and third iterations of the Marchenko scheme adaptively, as we did in Figure 6b. Note that the result of

Figure 7b has been obtained without resolving the multiple-generating boundaries in the overburden.

Conclusion

We have demonstrated how upgoing and downgoing wavefields in the subsurface can be retrieved by solving the multidimensional Marchenko equation. This can be done at any focal point individually, without having to resolve the overburden. The methodology has similarities with other data-driven methods for internal multiple elimination, in the sense that multiple multidimensional crosscorrelations are applied with the recorded data. Unlike in these other methods, a truncation is applied at the one-way traveltime of the direct wavefield after each iteration. To compute these one-way traveltimes, we make use of a macrovelocity model. As an imaging condition, we can apply either multidimensional deconvolution of the upgoing wavefield with the downgoing wavefield or crosscorrelation of the upgoing wavefield with the direct (downgoing) wavefield. Although artifacts from internal multiples are eliminated in both cases, the information content that internal multiples could add to the final image is not used when we use this crosscorrelation-based imaging condition. However, because the internal multiples of the downgoing wavefield are not required for this strategy and the upgoing wavefield can be retrieved adaptively, this gives the freedom to remove the artifacts from internal multiples by adaptive subtraction, as
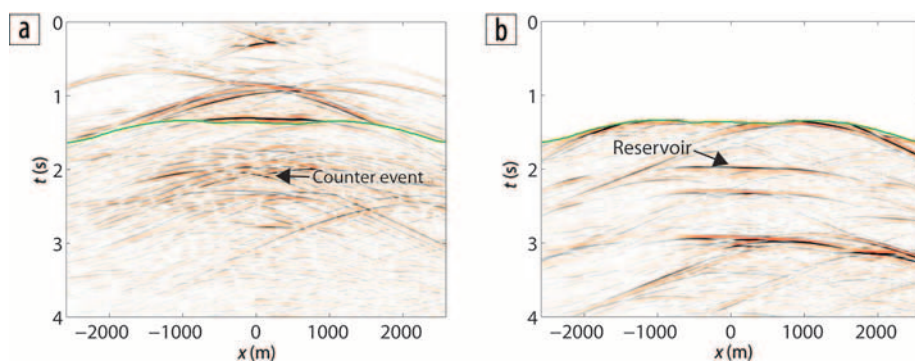

Figure 6. (a) Predicted update to the upgoing wavefield in Figure 4a, retrieved at the third iteration of the Marchenko scheme. (b) Adaptive addition of Figures 4a and 6a, in which all information before the truncation time has been removed.
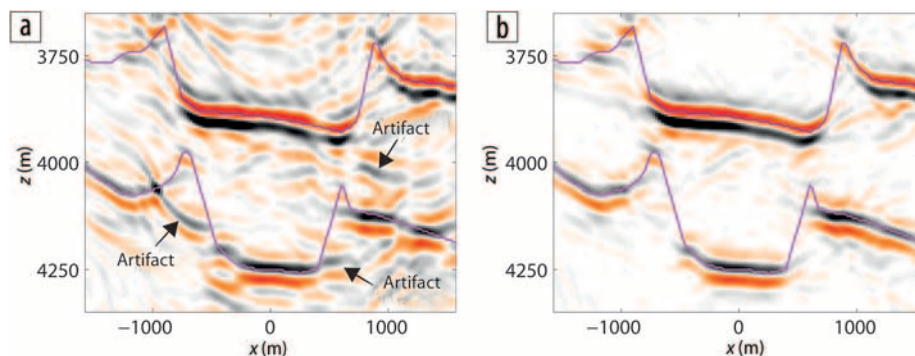

Figure 7. (a) Reverse time migration image of the target area shown in Figure 1a. (b) Improved RTM image in which inverse-wavefield extrapolation has been replaced by adaptively adding the first and third iterations of the Marchenko scheme. Magenta lines indicate true locations of the discontinuities, as computed directly from the model.

we have illustrated with a synthetic example. Care should be taken, however, when these artifacts interfere with physical reflections because the minimum-energy criterion that undergirds adaptive subtraction is not always satisfied. The individual updates of the upgoing wavefields also can be migrated individually and subtracted adaptively in the image domain. In any way, adaptive subtraction is likely to make Marchenko imaging more robust in the presence of background noise, attenuation, inaccurate source-signature deconvolution, ghosts, and variations in source/receiver coupling. **TLE**

Acknowledgments

Corresponding author: j.r.vanderneut@tudelft.nl

References

Behura, J., K. Wapenaar, and R. Snieder, 2014, Autofocus imaging: Image reconstruction based on inverse scattering theory: Geophysics, **79**, no. 3, A19–A26, http://dx.doi.org/10.1190/geo2013-0398.1.

Broggini, F., R. Snieder, and K. Wapenaar, 2012, Focusing the wavefield inside an unknown 1D medium: Beyond seismic interferometry: Geophysics, **77**, no. 5, A25–A28, http://dx.doi.org/10.1190/geo2012-0060.1.

Schuster, G. T., 2002, Reverse time migration = generalized diffraction stack migration: 72nd Annual Meeting, SEG, Expanded Abstracts, 1280–1283, http://dx.doi.org/10.1190/1.1816888.

van der Neut, J., I. Vasconcelos, and K. Wapenaar, 2014, An interferometric interpretation of Marchenko redatuming: 76th Conference and Exhibition, EAGE, Extended Abstracts, http://dx.doi.org/10.3997/2214-4609.20141369.

Wapenaar, K., J. Thorbecke, J. van der Neut, F. Broggini, E. Slob, and R. Snieder, 2014, Marchenko imaging: Geophysics, **79**, no. 3, WA39–WA57, http://dx.doi.org/10.1190/geo2013-0302.1.

Weglein, A. B, F. A. Gasparotto, P. M. Carvalho, and R. H. Stolt, 1997, An inverse-scattering series method for attenuating multiples in seismic reflection data: Geophysics, **62,** no. 6, 1975-1989, http://dx.doi.org/10.1190/1.1444298.

Special Section: Multiples from attenuation to imaging